unfractionated GFP-positive bone marrow cells (2×10^6 cells/mice) were injected intravenously via tail veins into 6-week-old female B6 mice after lethal doses (10 Gy) of whole-body γ-irradiation. At week 6 after bone marrow transplantation, viable GFP-positive bone marrow chimeric cells were confirmed by flow cytometry of peripheral blood. Only mice with greater than 90 percent GFP-positive white blood cells (CD45-positive cells) were used for further study. After bone marrow transplantation (week 8), inguinal fat pads of B6 mice were transplanted beneath scalps of GFPBM-B6 mice (B6→GFPBM-B6) (Fig. 1). Transplanted fat was then harvested 12 weeks after grafting.

Immunohistochemistry

Graft samples were fixed (Zinc Fixative; BD Biosciences, San Jose, Calif.), embedded in paraffin, and sectioned at 6 μm. The following primary antibodies were used: rabbit anti-GFP (Novus Biologicals, Littleton, Colo.), guinea pig anti-perilipin (Progen, Heidelberg, Germany), and rat anti-MAC-2 (Cedarlane Laboratories, Burlington, Ontario, Canada). Isotypic antibodies served as negative controls for each marker. Secondary antibodies (anti-rabbit Alexa Fluor 488 or anti-guinea pig Alexa Fluor 568) were applied as appropriate. Nuclei and vascular endothelial cells were delineated by Hoechst 33342 (Dojindo, Tokyo, Japan) and Alexa Fluor 647–conjugated lectin (Life Technologies Corp., Carlsbad, Calif.), respectively. Sections were examined via fluorescence (Keyence, Osaka, Japan) or confocal (TCS SP2 system; Leica, Heerbrugg, Switzerland) microscopy.

Whole-Mount Staining

Staining of fresh whole-mount tissue samples was also carried out, as described previously.[9] Briefly, 3-mm sections of adipose tissue were incubated for 30 minutes at 37°C with Alexa Fluor 568–conjugated or 647-conjugated lectin (Life Technologies), targeting vascular endothelial cells, and Hoechst 33342 (Dojindo), directed at nuclei. GFP was detectable without staining. Washed samples were examined via confocal microscopy (Leica TCS SP2 system). Serial images were recorded at 1-μm intervals, producing surface-rendered three-dimensional images.

Stromal Vascular Fraction Isolation

Adipose tissue was minced into 1-mm pieces and digested in phosphate-buffered saline plus 0.075 percent collagenase (Wako Pure Chemical Industries, Ltd., Osaka, Japan) for 30 minutes on a shaker at 37°C. Solutes were then washed, filtered (100-μm and 30-μm mesh), and centrifuged (800 *g* for 5 minutes). Erythrocytes were extracted using lysis buffer (Sigma Aldrich).

Portions of stromal vascular fraction cells were cultured in M199 medium (GIBCO Invitrogen, Carlsbad, Calif.) containing 10% fetal bovine serum, 100 IU of penicillin, 100 mg/ml streptomycin, 5 μg/ml heparin, and 2 ng/ml fibroblast growth factor-1. Contaminants, such as leukocytes and vascular endothelial cells, disappeared after passaging, and only adipose-derived stem/stromal cells were selectively expanded.[17] Adipose-derived stem/stromal cells at second passage were examined under fluorescence microscopy (Keyence) to ascertain GFP-positive cells.

Flow Cytometry Analysis

Stromal vascular fraction cells were identified by surface marker expression via flow cytometry, harvesting stromal vascular fraction cells of three mice for each experiment; analyses were performed in triplicate. Cells were incubated with rat anti-CD34-biotin antibodies (eBioscience, San Diego, Calif.) at 4°C for 30 min. After a wash with phosphate-buffered saline, the following secondary antibody and monoclonal antibody–fluorescein conjugates were applied at 4°C for 30 min: rat anti-streptoavidin-allophycocyanin, rat anti-CD31-fluorescein phycoerythrin (BD Bioscience), and rat anti-CD45-phycoerythrin Cy7 (eBioscience). GFP was detectable without staining. Cells were then analyzed using an LSR II flow cytometry system (BD Biosciences). Adipose-derived stem/stromal cells and vascular endothelial cells were determined as $D45^-/CD34^+/CD31^-$ cells and $CD45^-/CD34^+/CD31^+$ cells, respectively. Inguinal fat pads of normal GFP and B6 mice were also monitored as controls.

There were 4.6 ± 1.9 percent false-positives in B6 mice and 24.0 ± 1.1 percent false negatives in GFP mice (**see Figure, Supplemental Digital Content 1**, which shows a representative flow cytometric analysis of six varied samples. Adipose-derived stem/stromal cells and vascular endothelial cells were determined as $CD45^-/CD34^+/CD31^-$ cells and $CD45^-/CD34^+/CD31^+$ cells, respectively, ***http://links.lww.com/PRS/B296***). Data initially recorded were corrected as follows: *Corrected proportion* [percent] = 100 × (*Naïve data percent – GFP percent of B6 mice*) / (*GFP percent of GFP mice – GFP percent of B6 mice*).

Statistical Analysis

Results are expressed as median (quartile 1 to quartile 3). The Mann-Whitney test was used for

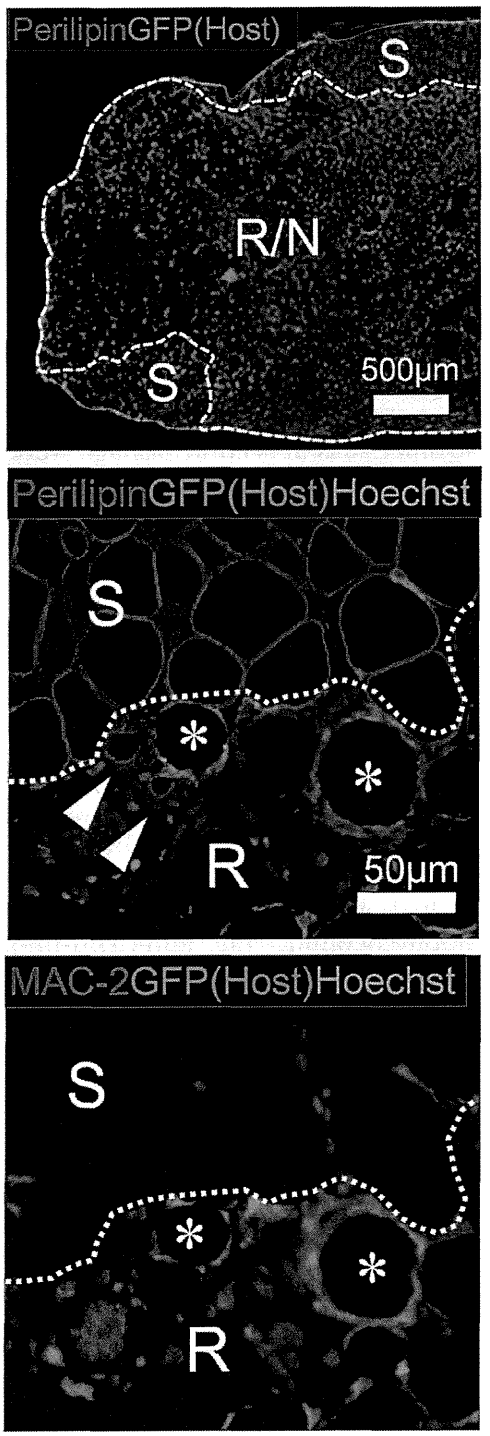

Fig. 2. Adipocyte degeneration/regeneration and host-cell infiltration. Immunostained sequential sections of inguinal fat at 1 week after transplantation are shown. (*Above*) The yellow interrupted line marks the border of surviving (*S*; perilipin-positive) and regenerating/necrotizing (*R/N*; perilipin-negative) tissue. Adipocytes undergo zonal necrosis resulting from ischemia, whereas superficial cells remain viable through plasmatic diffusion from peripheral host tissue. Infiltrating host cells (GFP-positive) predominate in regenerating areas. *Bar* = 500 μm. Sections of B6→GFP model stained for perilipin (adipocyte marker; *center*) and MAC-2 (macrophage marker; *below*) with Hoechst stain and GFP, respectively. Surviving (*S*) and regenerating (*R*) zones of adipocytes are clearly demarcated by perilipin staining (*dotted line*). Host cells infiltrated regenerating areas only and were mostly MAC-2-positive macrophages. The *asterisk* indicates crown-like structure (necrotic adipocytes rimmed by phagocytic macrophages). *Arrowheads* highlight graft-derived (GFP-negative) regenerating adipocytes. *Bars* = 50 μm. (*Below*) MAC-2-positive cells quantified relative to all host cells. Nonmacrophage host cells (MAC-2$^-$/GFP$^+$) rose in number over time. Data are expressed as median (quartile 1 to quartile 3).

two-group comparisons. Bonferroni correction was used for multiple testing. Statistical significance was otherwise set at $p < 0.05$.

RESULTS

Tissue Regeneration/Remodeling after Fat Grafting

In both exchange models (B6→GFP and GFP→B6), normalized weights of inguinal fat grafts reduced over time since 2 weeks after grafting and was approximately one-half of control at 12 weeks. The graft weight of respective models did not differ statistically at either time point. [**See Figure, Supplemental Digital Content 2**, which shows sequential changes in normalized graft weight of both fat exchange models. Weights of graft samples were normalized, dividing sample weight by body weight. Normalized weight ratios did not differ significantly by graft model (B6→GFP versus GFP→B6). Data are expressed as median (quartile 1 to quartile 3), ***http://links.lww.com/PRS/B297***.]

Grafted adipose tissue underwent total tissue remodeling, as we reported previously.[12,13] Immunohistochemistry of B6→GFP and GFP→B6 models revealed localization of host-derived and graft-derived cells (GFP-positive cells), respectively. With the exception of the most superficial perilipin-positive survival zone (100 to 500 μm from graft surface), all adipocytes were necrotic (perilipin-negative) by 1 week (Fig. 2, *above*). F2
Perilipin is a protein that coats lipid droplets in adipocytes and is detectable only in viable adipocytes.[12] Regenerating and necrotizing zones were then partly replaced by resident and infiltrating stem/progenitor cells. The adipocyte regeneration was complete by 12 weeks.

At 1 week, numerous host cells infiltrated in regenerating/necrotizing perilipin-negative zones but not the viable perilipin-positive survival zone (Fig. 2, *center*). Sequential sections showed that infiltrating host cells were primarily

MAC-2–positive macrophages, and crown-like structures (necrotic adipocytes rimmed by macrophages) were noted (Fig. 2, *below*). Small (<30 μm), regenerative, perilipin-positive adipocytes were also observed at the peripheries of regenerating zones. Temporal quantification of cell types confirmed that host cells were mainly MAC-2–positive macrophages (Fig. 3), which peaked at F3 2 weeks (>90 percent) and later declined [62.6 percent (range, 56.3 to 69.9 percent) at 12 weeks; $n = 3$]. At completion of regeneration (12 weeks), scavenging of oil drops was still in progress.

Immunohistologic Assessment of Regenerated Adipocytes

Origins of cells in regenerated adipose tissue were assessed in grafted samples at 12 weeks, with a focus on adipocytes, vessel wall structures, capillaries (vascular endothelial cells), and adipose-derived stem/stromal cells.

In sections of the B6→GFP model, perilipin-negative areas (oil drops) were surrounded by GFP-positive macrophages. However, regenerating perilipin-positive adipocytes barely expressed GFP, suggesting that most of the adipocytes were F4 of graft origin (Fig. 4, *above*). This was corroborated by sections of the GFP→B6 model, in which nearly all perilipin-positive adipocytes expressed GFP (the graft marker here) (Fig. 4, *below*). Furthermore, host-derived adipocytes (GFP-positive/perilipin-negative cells in the B6→GFP model; GFP-negative/perilipin-positive cells in the GFP→B6 model) were exceedingly rare (Fig. 4, *below*), and GFP-positive adipocytes were undetectable in the B6→GFPBM-B6 model. Thus, nearly all regenerated adipocytes were derived from adipocyte progenitors (adipose-derived stem/stromal cells) in grafted tissue, with negligible host-derived contributions.

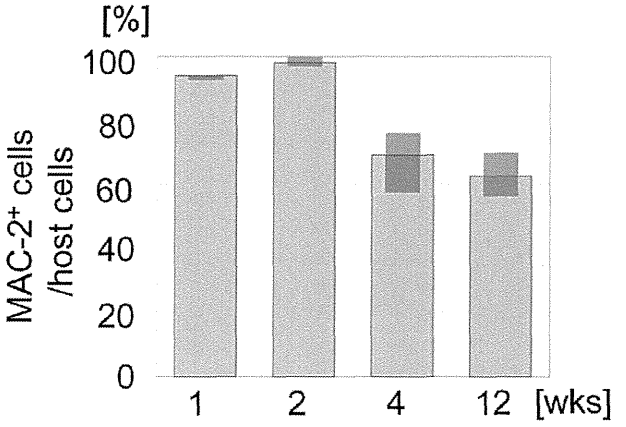

AQ6 **Fig. 3.** MAC-2-positive cells quantified relative to all host cells. Nonmacrophage host cells (MAC-2⁻/GFP⁺) rose in number over time. Data are expressed as median (quartile 1 to quartile 3).

Immunohistologic Assessment of Vessel Wall Cells and Capillaries

Large vessels were identified morphologically under phase contrast imaging, and vascular wall smooth muscle cells were evaluated via immunohistochemistry. Host-derived cells accounted for 15.4 percent (range, 11.7 to 17.5 percent) in B6→GFP samplings ($n = 9$) and 36.0 percent (range, 26.1 to 41.8 percent) in GFP→B6 samplings ($n = 9$), indicating a predominance of graft-derived cells (Fig. 5). F5

Stained whole-mount samples clearly showed that graft-derived and host-derived cells were equally represented in chimeric capillaries of both B6→GFP and GFP→B6 models (Fig. 6, *above* and F6 *center*). This was confirmed by immunostained sections. To further investigate the contribution of host bone marrow–derived cells, whole-mount samples of the B6→GFPBM-B6 model were also stained. Chimeric capillaries, formed through contributing host bone marrow–derived cells (Fig. 6, *below*), were similarly seen.

Flow Cytometric Analysis of Stromal Vascular Fraction

GFP-positive cells were quantified by flow cytometry of stromal vascular fraction cells (i.e., fat constituents other than adipocytes), isolated through collagenase digestion of graft samples. Adipose-derived stem/stromal cells and vascular endothelial cells were identified as $CD45^-/CD34^+/CD31^-$ cells and $CD45^-/CD34^+/CD31^+$ cells, respectively. Representative data of six samples (B6, GFP, B6→GFP, GFP→B6, GFPBM-B6, and B6→GFPBM-B6) are shown in Figure 7 (*above*) F7 and in **Figure, Supplemental Digital Content 1**, ***http://links.lww.com/PRS/B296***. Initial flow cytometry data were corrected as described (see Materials and Methods), and resultant data on cellular origins are shown in Figure 7 (*center*). Our findings suggest that adipose-derived stem/stromal cells were both graft-derived and host-derived, and that host-derived adipose-derived stem/stromal cells were similarly of bone marrow and non–bone marrow derivation. Therefore, surrounding recipient tissue likely supplied some adipose-derived stem/stromal cells during the process of regeneration. Vascular endothelial cells were also composed of graft and host cells to a similar extent, but the host contribution was mostly from bone marrow, with a negligible non–bone marrow component.

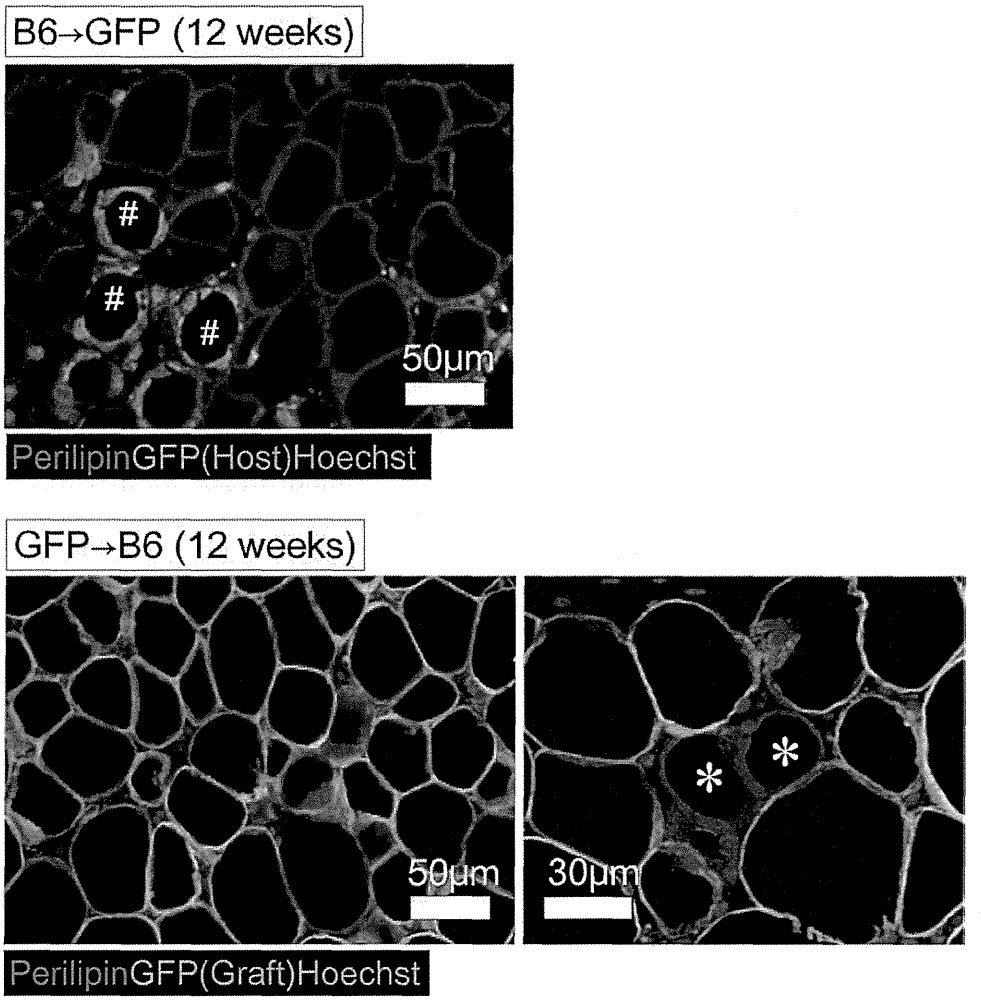

Fig. 4. Origin of regenerated mature adipocytes in exchanged fat. (*Above*) In the B6→GFP model, most mature adipocytes (perilipin-positive) at 12 weeks are GFP-negative (graft-derived). GFP-positive cells surrounding oil drops (#) are chiefly macrophages. *Bars* = 30 μm. (*Below*) In the GFP→B6 model, most mature adipocytes (perilipin-positive) at 12 weeks are GFP-positive (graft-derived) and thus appear yellow (*left*). Host-derived adipocytes (perilipin-positive/GFP-negative) (*) are very rarely detected (*right*). *Bar* = 50 μm (*left*) and 30 μm (*right*).

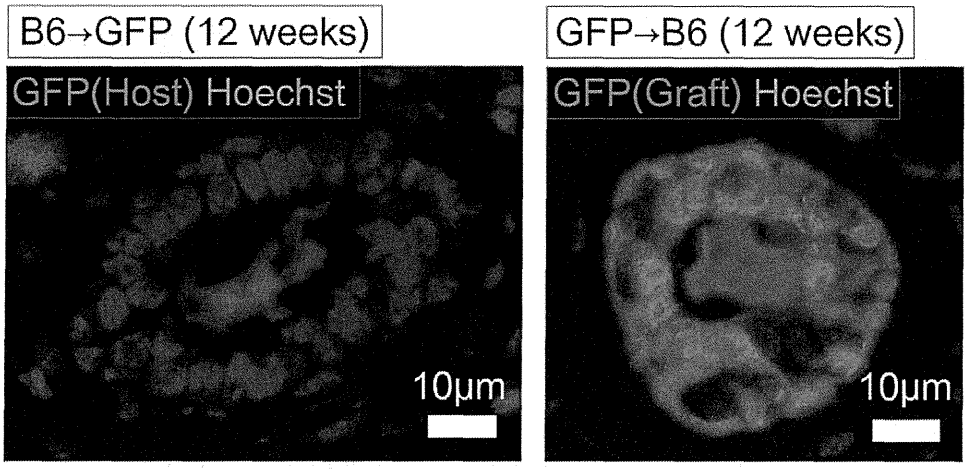

AQ7

Fig. 5. Origin of vessels and capillaries in exchanged fat tissue. Large vessels chiefly incorporated graft-derived smooth muscle cells in both B6→GFP (*left*) and GFP→B6 (*right*) models. *Bar* = 10 μm.

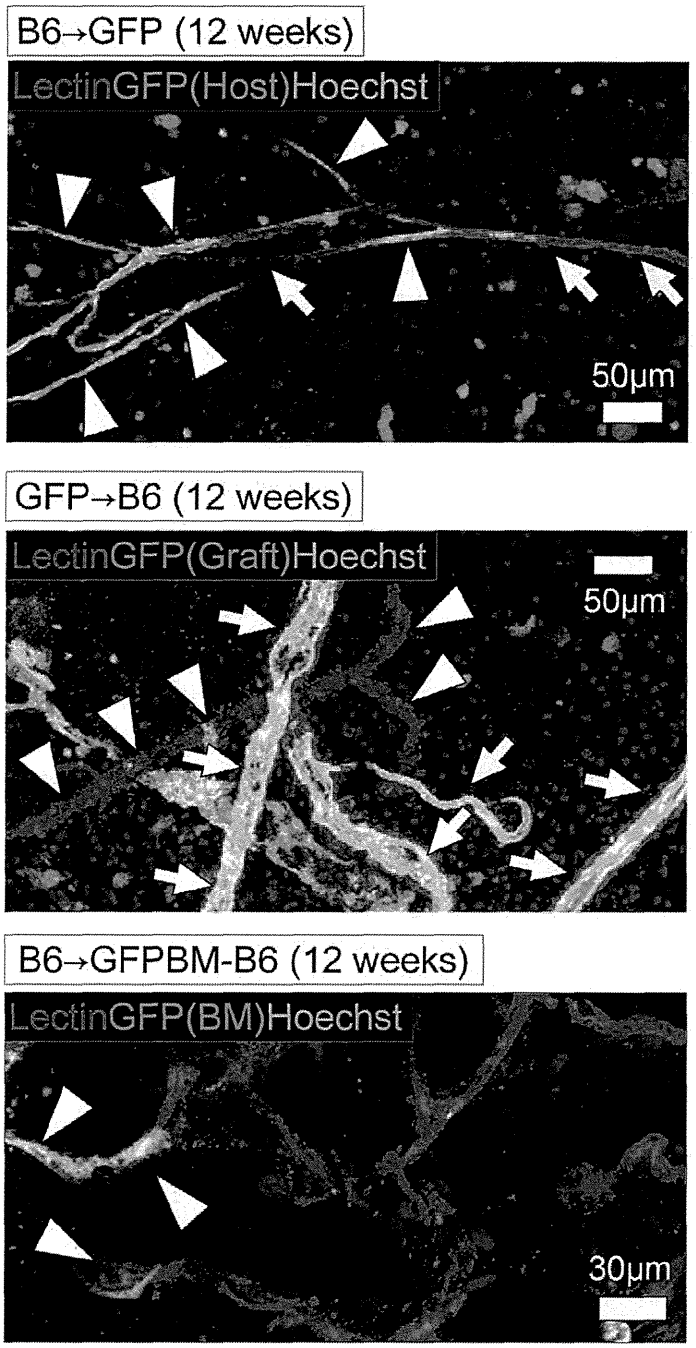

Fig. 6. Origin of vessels and capillaries in exchanged fat tissue. Stained whole-mount samples of B6→GFP (*above*) and GFP→B6 (*center*) models show graft/host chimeric capillaries. *Arrows* indicate graft-derived vascular endothelial (lectin-positive) cells; *arrowheads* highlight host-derived endothelial cells. *Bar* = 50 μm. (*Below*) Stained whole-mount samples of the B6→GFPBM-B6 model showing lectin-positive/GFP-positive host bone marrow–derived vascular endothelial cells. *Bar* = 30 μm.

Stromal vascular fraction cells from B6→GFP and GFP→B6 samples were cultured (Fig. 7, *below, left*). Flow cytometric data of cultured adipose-derived stem/stromal cells were comparable to those of noncultured adipose-derived stem/stromal cells (Fig. 7, *below, right*). Host proportions were 67.7 percent (range, 62.7 to 80.0 percent $n = 3$) and 49.2 percent (range, 33.3 to 67.7 percent; $n = 3$)

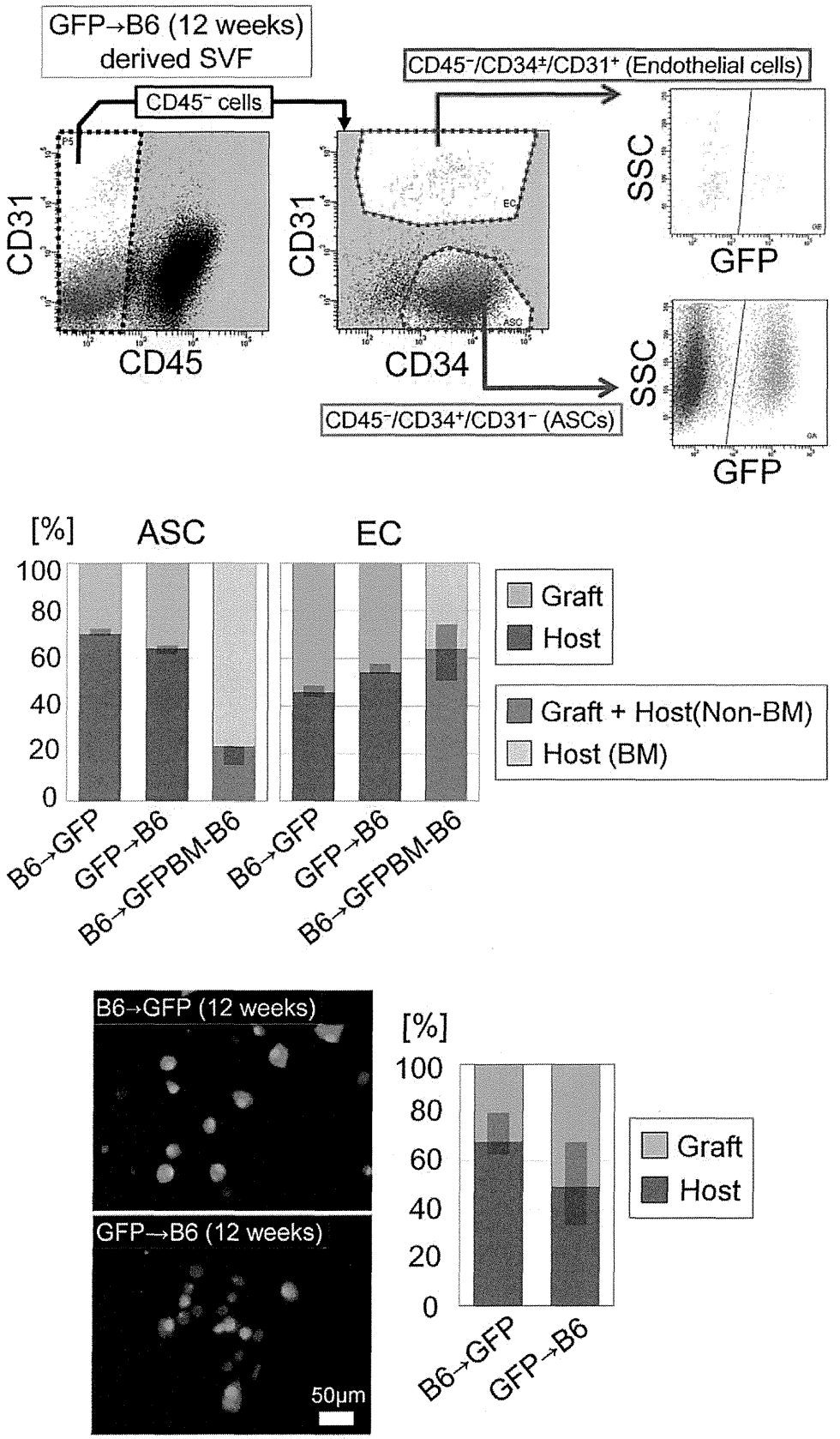

Fig. 7. Analysis of stromal vascular fraction cells isolated from exchanged fat. Freshly isolated or cultured stromal vascular fraction cells from fat samples (three each) of B6→GFP and GFP→B6 models analyzed at 12 weeks. Adipose-derived stem/stromal cells (*ASCs*) and vascular endothelial cells (*ECs*) were determined by flow cytometry ($CD45^-/CD34^+/CD31^-$ cells

in adipose-derived stem/stromal cells of B6→GFP and GFP→B6 models, respectively.

DISCUSSION

Our previous studies[12,13] suggested that adipose tissue is remodeled during the first 3 months, but the cellular origin of regenerated adipose tissue remained unknown. Using the histological and flow cytometrical data of this study, we summarized the origin of each cellular component in grafted/regenerated fat tissue in Table 1. Except for surviving adipocytes that were superficially located, all other adipocytes are supposed to be regenerated mostly from graft-resident adipose-derived stem/stromal cells. Most of the vascular mural cells are also derived from the graft, whereas nearly half of vascular endothelial cells originate from bone marrow of the host. Adipose-derived stem/stromal cells were a mixture of the graft, the host nonbone marrow, and the host bone marrow. The discrepancy in cellular origin between adipocytes and adipose-derived stem/stromal cells suggested that adipose-derived stem/stromal cells have to reside next to adipocytes to become adipocytes upon adipocyte death, although new adipocytes can be provided from surrounding tissue and bone marrow.

Tissue remodeling in grafted fat was initiated by zonal adipocyte necrosis, triggering adipose-derived stem/stromal cell activation and host cell infiltration by 1 week. Host-cell infiltrates at the early inflammatory phase of repair were almost exclusively macrophages, although by week 12 their percentage had declined to 60 percent, suggesting that other types of cells were involved in later phases of regeneration. Previously, we alluded to the differential roles of inflammatory (M1) macrophages and anti-inflammatory (M2) macrophages in the remodeling of fat.[13,14] M1 macrophages surround and phagocytize necrotic adipocytes (lipid droplets), whereas M2 macrophages appear to take part in scar/capsule formation.

Table 1. Origins of Cellular Components in Grafted Fat

		Host	
	Graft	Non–Bone Marrow	Bone Marrow
Adipocytes	++++	±	−
Vascular mural cells	+++	+	±
Vascular endothelial cells	++	±	++
Adipose-derived stem/stromal cells	++	++	++

Herein, the origins of cellular elements in grafted fat were evaluated at 12 weeks, which reportedly is the time interval required to complete the regeneration of grafts. However, phagocytosis and scar formation are still ongoing beyond this point. Outcomes of our fat exchange graft models clearly indicate the differential contribution of graft-derived and host-derived cells in regenerating/remodeling adipose tissue. New host-derived adipocytes (likely contributed by migrating adipose-derived stem/stromal cells of peripheral host tissue) were rarely detected. Instead, nearly all adipocytes originated from grafts alone. On the other hand (and interestingly), adipose-derived stem/stromal cells found in regenerated fat as future contributors to adipose remodeling were of graft and host origins. Flow cytometric analysis and our experimental bone marrow transplantation in mice suggested that not all host-derived adipose-derived stem/stromal cells originate from bone marrow. A substantial number of stem/progenitor cells likely migrated into grafts from local host tissue as well resided as adipose-derived stem/stromal cells in regenerated fat. Indeed, a previous report has shown that adipose tissue may even release adipose-derived stem/stromal cells into lymphatic flow, and this mobilization of adipose-derived stem/stromal cells may be controlled by CXCR4.[18]

The discrepancy between observed origins of adipocytes and adipose-derived stem/stromal cells is unexplained as yet. Some studies have suggested that bone marrow–derived cells (M2 macrophages) home to adipose tissue and may transform into adipose-derived stem/stromal cells,[19–21] and bone marrow-derived cells are capable of adipocyte differentiation under non-physiologic experimental conditions, such as a chamber neogenesis model.[22,23] Still, adipocytes

Fig. 7. (*Continued*) and $CD45^-/CD34^+/CD31^+$ cells, respectively). (*Above*) Representative flow cytometric data of stromal vascular fraction cells isolated from GFP→B6 sample at 12 weeks are shown. *SSC*, side scatter. (*Center*) Origins of adipose-derived stem/stromal cells and vascular endothelial cells in samples of B6→GFP, GFP→B6, and B6→GFPBM-B6 models. Flow cytometry confirmed that both adipose-derived stem/stromal cells and vascular endothelial cells were mixtures of graft-derived and host-derived cells. Host-contributed adipose-derived stem/stromal cells were both non–bone marrow– and bone marrow–derived, whereas host-contributed vascular endothelial cells were primarily bone marrow derivatives. Data are expressed as median (quartile 1 to quartile 3) ($n = 3$ at each time point). (*Below, left*) Cultured adipose-derived stem/stromal cells from samples of B6→GFP and GFP→B6 models under fluorescent microscope. (*Below, right*) Graft/host ratio of cultured adipose-derived stem/stromal cells. Data are expressed as median (quartile 1–quatile 3).

derived from bone marrow are rarely found in mice on normal or high-fat diets.[16,19] Nevertheless, our findings plainly indicate that adipose-derived stem/stromal cells in the grafted tissue are crucial for adipocyte regeneration after fat grafting.

In addition, we found that mural cells (vascular smooth muscle cells) were largely of graft derivation, whereas the origins of vascular endothelial cells were quite different. Both histologic and flow cytometric analyses revealed a mix of graft and host origins for these cells. Unlike adipose-derived stem/stromal cells, our experimental transplantation of mouse bone marrow suggested that nearly all host-derived vascular endothelial cells originate from bone marrow. This means that a substantial number of endothelial progenitor cells are mobilized from bone marrow, resulting in a capillary network chimera. Similar graft/host chimeric capillaries have been observed after kidney transplantation.[24] Hence, capillary remodeling in the aftermath of fat grafting technically is a culmination of vasculogenesis, rather than angiogenesis.

CONCLUSIONS

The clinical implications of this study are considerable in terms of homeostasis/remodeling in adipose tissue and repair/regeneration of grafted fat. Next-generation adipocytes in fat grafts are derived from adipose-derived stem/stromal cells in the graft, but new adipose-derived stem/stromal cells for future remodeling are also provided by bone marrow and other local (adipose) tissue elements. Adipose tissue may also serve as a reservoir of adipose-derived stem/stromal cells from circulation. Although graft-derived vascular structures are involved in revascularization after fat grafting, endothelial progenitor cells mobilized from bone marrow are major contributors as well. We believe that understanding the mechanisms of fat grafting would strategically improve current grafting procedures. Our findings also propose future studies that explore novel methods to manipulate activation, migration, or homing of graft-derived and bone marrow–derived stem/progenitor cells.

Kotaro Yoshimura, M.D.
Department of Plastic Surgery
University of Tokyo School of Medicine
7-3-1, Hongo, Bunkyo-Ku
Tokyo 113-8655, Japan
kotaro-yoshimura@umin.ac.jp

ACKNOWLEDGMENTS

This study was supported by the Japanese Ministry of Education, Culture, Sports, Science, and Technology (Grant-in-Aid for Scientific Research B3-24390398). The authors greatly appreciate the substantial contributions to this study by Drs. Kazuhide Mineda and Takanobu Mashiko. They also thank Ayako Sato for technical assistance.

REFERENCES

1. Eto H, Suga H, Matsumoto D, et al. Characterization of structure and cellular components of aspirated and excised adipose tissue. *Plast Reconstr Surg.* 2009;124:1087–1097.
2. Safford KM, Hicok KC, Safford SD, et al. Neurogenic differentiation of murine and human adipose-derived stromal cells. *Biochem Biophys Res Commun.* 2002;294:371–379.
3. Tholpady SS, Katz AJ, Ogle RC. Mesenchymal stem cells from rat visceral fat exhibit multipotential differentiation in vitro. *Anat Rec A Discov Mol Cell Evol Biol.* 2003;272:398–402.
4. Safford KM, Safford SD, Gimble JM, et al. Characterization of neuronal/glial differentiation of murine adipose-derived adult stromal cells. *Exp Neurol.* 2004;187:319–328.
5. Seo MJ, Suh SY, Bae YC, Jung JS. Differentiation of human adipose stromal cells into hepatic lineage in vitro and in vivo. *Biochem Biophys Res Commun.* 2005;328:258–264.
6. Yanez R, Lamana ML, Garcia-Castro J, et al. Adipose tissue-derived mesenchymal stem cells have in vivo immunosuppressive properties applicable for the control of the graft-versus-host disease. *Stem Cells* 2006;24:2582–2591.
7. Casteilla L, Planat-Benard V, Laharrague P, et al. Adipose-derived stromal cells: Their identity and uses in clinical trials, an update. *World J Stem Cells.* 2011;3:25–33.
8. Gimble JM, Guilak F, Bunnell BA. Clinical and preclinical translation of cell-based therapies using adipose tissue-derived cells. *Stem Cell Res Ther.* 2010;1:19. AQ9
9. Suga H, Eto H, Shigeura T, et al. IFATS collection: Fibroblast growth factor-2-induced hepatocyte growth factor secretion by adipose-derived stromal cells inhibits postinjury fibrogenesis through a c-Jun N-terminal kinase-dependent mechanism. *Stem Cells* 2009;27:238–249.
10. Kato H, Suga H, Eto H, et al. Reversible adipose tissue enlargement induced by external tissue suspension: Possible contribution of basic fibroblast growth factor in the preservation of enlarged tissue. *Tissue Eng Part A* 2010;16:2029–2040.
11. Suga H, Eto H, Aoi N, et al. Adipose tissue remodeling under ischemia: Death of adipocytes and activation of stem/progenitor cells. *Plast Reconstr Surg.* 2010;126:1911–1923.
12. Eto H, Kato H, Suga H, et al. The fate of adipocytes after nonvascularized fat grafting: Evidence of early death and replacement of adipocytes. *Plast Reconstr Surg.* 2012;129:1081–1092.
13. Kato H, Mineda K, Eto H, et al. Degeneration, regeneration, and cicatrization after fat grafting: Dynamic total tissue remodeling during the first 3 months. *Plast Reconstr Surg.* 2014;133:303e–313e.
14. Mineda K, Kuno S, Kato H, et al. Chronic inflammation and progressive calcification as a result of fat necrosis: The worst end in fat grafting. *Plast Reconstr Surg.* 2014;133:1064–1072.
15. Dimarino AM, Caplan AI, Bonfield TL. Mesenchymal stem cells in tissue repair. *Front Immunol.* 2013;4:201. AQ10
16. Tomiyama K, Murase N, Stolz DB, et al. Characterization of transplanted green fluorescent protein+ bone marrow cells into adipose tissue. *Stem Cells* 2008;26:330–338.
17. Yoshimura K, Shigeura T, Matsumoto D, et al. Characterization of freshly isolated and cultured cells derived from the fatty and fluid portions of liposuction aspirates. *J Cell Physiol.* 2006;208:64–76.

18. Gil-Ortega M, Garidou L, Barreau C, et al. Native adipose stromal cells egress from adipose tissue in vivo: Evidence during lymph node activation. *Stem Cells* 2013;31:1309–1320.
19. Crossno JT Jr, Majka SM, Grazia T, et al. Rosiglitazone promotes development of a novel adipocyte population from bone marrow-derived circulating progenitor cells. *J Clin Invest.* 2006;116:3220–3228.
20. Hausman GJ, Hausman DB. Search for the preadipocyte progenitor cell. *J Clin Invest.* 2006;116:3103–3106.
21. Eto H, Ishimine H, Kinoshita K, et al. Characterization of human adipose tissue-resident hematopoietic cell populations reveals a novel macrophage subpopulation with CD34 expression and mesenchymal multipotency. *Stem Cells Dev.* 2013;22:985–997.
22. Stillaert F, Findlay M, Palmer J, et al. Host rather than graft origin of Matrigel-induced adipose tissue in the murine tissue-engineering chamber. *Tissue Eng.* 2007;13:2291–2300.
23. Lee YH, Petkova AP, Granneman JG. Identification of an adipogenic niche for adipose tissue remodeling and restoration. *Cell Metab.* 2013;18:355–367.
24. Lagaaij EL, Cramer-Knijnenburg GF, van Kemenade FJ, et al. Endothelial cell chimerism after renal transplantation and vascular rejection. *Lancet.* 2001;357:33–37.

AUTHOR QUERIES

AUTHOR PLEASE ANSWER ALL QUERIES

AQ1—Please provide the hightest degree earned for all authors.

AQ2—GFP spelled out correctly as "green fluorescent protein"? If not, please provide the correct expansion.

AQ3—It looks like ref 15 is meant here, rather than ref 18 as in original manuscript. Okay to cite ref 15 here? If not, please cite ref 15 in text where wanted, renumbering as needed so that refs are cited in numerical order, per Journal style.

AQ4—GFP defined correctly as "green fluorescent protein"? If not, please provide the correct definition.

AQ5—Please provide name and city/state location of manufacturer of Alexa Fluor secondary antibodies, per Journal style for use of brand names.

AQ6—Original Figure 2 was divided into Figures 2 and 3 by the editorial office, and subsequent figures were renumbered accordingly. Please confirm that figure legends are correct as divided/edited.

AQ7—Original Figure 4 was divided into Figures 5 and 6. Legends correct as edited? Please advise/revise as needed.

AQ8—Figure panels correct as described in the legend to Figure 7 (i.e., "Below, left" and "Below, right")? If not, please revise as needed.

AQ9—Please supply ending folio for ref 8, for a complete page range.

AQ10—Please supply ending folio for ref 15, for a complete page range.

AQ11—Please confirm that disclosure statement is correct as edited. Grant information has been moved to the Acknowledgments section, per Journal style.

Short Communication

For reprint orders, please contact: reprints@futuremedicine.com

Regenerative Medicine

Micronized cellular adipose matrix as a therapeutic injectable for diabetic ulcer

Jingwei Feng[‡,1], Kentaro Doi[‡,1], Shinichiro Kuno[1], Kazuhide Mineda[1], Harunosuke Kato[1], Kahori Kinoshita[1], Koji Kanayama[1], Takanobu Mashiko[1] & Kotaro Yoshimura*[,1]

[1]Departments of Plastic Surgery, University of Tokyo Graduate School of Medicine, 7-3-1, Hongo, Bunkyo-Ku, Tokyo 113-8655, Japan

*Author for correspondence:
Tel: +81 3 5800 8948
Fax: +81 3 5800 8947
kotaro-yoshimura@umin.ac.jp

[‡]Authors contributed equally

Background: Despite the clinical potential of adipose-derived stem/stromal cells (ASCs), there are some clinical difficulties due to the regulation of cell therapies. **Materials & methods:** Micronized cellular adipose matrix (MCAM) injectable was prepared through selective extraction of connective tissue fractions in fat tissue only through mechanical minimal manipulation procedures. **Results:** It retained some capillaries and ASCs, but most adipocytes were removed. The presence of viable ASCs, vascular endothelial cells was confirmed and ASCs of MCAM kept intact mesenchymal differentiation capacity. In diabetic mice, skin wounds treated with MCAM showed significantly accelerated healing compared with phosphate-buffered saline-treated ones. **Conclusion:** The proven potential of MCAM to accelerate healing in ischemic diabetic ulcers may offer a simple, safe and minimally invasive means for tissue repair and revitalization.

Keywords: adipose stem cells • diabetic ulcer • extracellular matrix • flow cytometry • ischemia • lipoaspirates • minimal manipulation • tissue revitalization • vascular endothelial cells • wound healing

Adipose tissue is structurally complex, harboring a variety of cells within its lobulated fibrous septal network. Through enzymatic digestion, this network can be disintegrated and its heterogeneous complement of indigenous cells, or so called stromal vascular fraction (SVF), may be isolated. Because adipose-derived stem/stromal cells (ASCs) are important SVF residents with mesenchymal multipotency [1,2], SVF has been strategically engaged as a supplement to enhance fat engraftment [1,3–4]. However, if dissociated SVF cells are injected separately, rather than properly integrated into grafted fat, unexpected migratory and/or phenotypic outcomes may result, creating adverse complications (i.e., ectopic fibrosis and lymphadenopathy) [5]. Currently, a number of vehicles for delivery of cells are available, such as injectable biomaterial scaffolds, 3D spheroidal cell cultures and engineered cell sheets [6–8]. These sophisticated constructs help prevent untoward cell migration, thus avoiding lost or undesired contributions by cellular and extracellular matrix (ECM) componentry.

Decellularized ECM of various tissues or organs may serve as bioactive scaffolding, thereby facilitating tissue remodeling and repair [9–11]. Although adipocytes account for >90% of fatty tissue by volume, the native ECM of fat provides a niche for other cellular subsets (e.g., ASCs, vascular endothelial cells and pericytes), enabling biologic functions that are shared in part with acellular dermal matrix.

As niche components, stem cells generally lie in wait for changes in microenvironment. Stem cells isolated from the tissue, however, are already activated in an unphysiological microenvironment, and thus extra care needs to be taken in controlling the fate and behaviors of those cells in clinical utilization. Since 2005, policies of the US FDA aimed at preventing potential contamination and genetic alteration of

Future Medicine part of fsg

stem cells [12] and enzymatic isolation and cultural expansion of ASCs were not considered as 'minimal manipulation', although isolated or cultured ASCs are already extensively used in a number of clinical trials.

For this investigation, a bioactive injectable comprised of functional ECM and resident cells (including ASCs) was formulated through minimal manipulation of adipose tissue. Given the combination of micronized connective tissue, viable ASCs and vascular endothelial cells generated, we have applied the term micronized cellular adipose matrix (MCAM). In this study, injectable MCAM was tested for its therapeutic value for wound repair of diabetic skin ulcer. Wound healing impairment in diabetic patients is a significant clinical issue affecting millions of patients worldwide. The major underlying pathology is noted to be chronic inflammation and ischemia based on peripheral vascular dysfunction, where tissue-resident stem cells are considered to be depleted. Although numerous products for wound dressing with bioactive ECM or growth factors are available, the clinical effects on diabetic ulcer are very limited. Thus, we sought to characterize and evaluate MCAM, which contains human adipose derived stem cells and vascular endothelial cells in their original niche of ECM, as a potential therapeutic tool for stem cell-depleted pathological conditions.

Materials & methods

Mouse tissue preparation

C57BL/6JJcL mouse inguinal fat pads were harvested, washed and weighed. One gram of fat pads was cut into tiny pieces with surgical scissors (continuous fine mincing for 5 min). After transfer to a tube containing 2.5 ml cooled phosphate-buffered saline (PBS), the morcellated tissue was thoroughly shaken several times and then centrifuged (800 × *g*, 5 min). MCAM was extracted as tissue sediment, and floating fatty tissue was also sampled.

Human tissue preparation

Lipoaspirate was obtained from a healthy 23-year-old female donor (BMI = 24) submitting to abdominal liposuction under general anesthesia. The study protocol was approved by our Institutional Review Board. Once soft tissues were infiltrated with a solution of saline plus epinephrine (1:1,000,000), subcutaneous fat was suctioned (-500 to -700 mmHg) using a conventional liposuction machine equipped with a 2.5-mm (inner diameter) cannula. MCAM was extracted from the lipoaspirate with the above described micronization and centrifugation, and floating fat was also sampled.

Whole-mount staining

Whole-mount staining was performed with Wheat germ agglutinin (WGA) Alexa Fluor 488 (Life Technologies, CA, USA), lectin PNA Alexa Fluor 594 (Life Technologies) and Hoechst 33342 solution (Dojindo, Kumamoto, Japan) as instructed by manufacturers. Images were then acquired via confocal microscope (Leica DMIRE2; Leica Microsystems, Wetzlar, Germany).

Flow cytometry

Mouse MCAM and roughly excised inguinal fat were separately prepared. Each sample was digested in 0.1% collagenase (Wako, Osaka, Japan) Hank's balanced salt solution (HBSS) by incubation in a shaking water bath (37°C, 30 min). To remove the collagenase, SVF cells were washed with PBS for three-times. After filtration, SVF cells were washed and stained with the following antibodies and corresponding isotype controls: Anti-CD45-Viogreen (Miltenyi Biotec, Bergisch Gladbach, Germany), Anti-CD34-Biotin (eBioscience, Inc., CA, USA), Rat IgG2a Kappa Control Biotin (BD Biosciences, CA, USA), Streptavidin-APC (BD Biosciences), Anti-CD31-PE (BD Biosciences), Rat IgG2a Kappa Control PE (BD Biosciences). Samples and controls were then analyzed by flow cytometry (MACSQuant Analyzer 10; Miltenyi Biotec). Gating for each signal was set to eliminate 99.9% of the cells in corresponding isotype control. CD45 gating was applied first, and CD45-negative portion was further analyzed for CD34 and CD31 signals.

Cultured ASCs of human origin

Human ASCs in floating fat and in MCAM were cultured separately. Floating fat was digested with collagenase (as above) [12], and isolated SVF cells were seeded in Dulbecco's Modified Eagle Media (DMEM), supplemented with 10% fetal bovine serum (FBS), 100 IU penicillin and 100 mg/ml streptomycin. Explant culture was performed for human MCAM to generate MCAM-derived ASCs.

Multilineage differentiation assay

Assays of adipogenic, osteogenic and chondrogenic lineages were conducted as follows: adipogenic differentiation: ASCs were incubated for 21 days in DMEM containing 10% FBS, 0.5 mM isobutyl-methyl-xanthine, 1 M dexamethasone, 10 µM insulin and 200 µM indomethacin; osteogenic differentiation: ASCs were incubated for 21 days in DMEM containing 10% FBS supplemented with 0.1 mM dexamethasone, 50 mM ascorbate-2-phosphate and 10 mM glycerophosphate (Nacalai Tesque Inc, Kyoto, Japan); and chondrogenic differentiation: a micromass culture system was

utilized, as previously reported [13], incubating ASCs in a 15 ml tube for 21 days in DMEM containing 1% FBS supplemented with 6.25 mg/ml insulin, 10 ng/ml TGFβ-1 and 50 nM of ascorbate-2-phosphate. Regular growth medium was used to plate controls. The three lineages were analyzed qualitatively via Nile red (adipogenic), von Kossa (osteogenic) and Alcian blue (chondrogenic) differential staining and gauged quantitatively by AdipoRed assay (Lonza, Basel, Switzerland), Calcium-E test (Wako Pure Chemical Industries Ltd, Osaka, Japan) and micromass diameter.

Healing of diabetic ulcers in mice models

Care of B6-db/db mice (BKS.Cg/Lepr^{db}/m/JCL, 8-week old male) was conducted in accordance with institutional guidelines, using a protocol approved by the Animal Experimental Committee of University of Tokyo. Under general anesthesia (isoflurane inhalation), the B6-db/db mice were depilated and two full-thickness cutaneous wounds (6 mm each) were created on both sides dorsally, using skin punch devices. A donut-shaped silicone splint was then placed to prevent wound contraction and secured by interrupted 6–0 nylon sutures. MCAM prepared from one inguinal fat pad of a wild-type B6 mouse was injected by 29-G needle into four differing points of subcutis at wound peripheries (n = 4). Injection of PBS served as control. Treated wounds and splints were covered by transparent sterile dressings. Wounds were photographed on days 0, 2, 4, 7, 9, 11 and 14, determining their areas by Photoshop CS5 (Adobe Systems, CA, USA).

Statistical analysis

Results were expressed as mean ± standard error of the mean. To compare capacity for multilineage differentiation, Student's *t*-test was applied; and paired *t*-test was invoked for comparing wound sizes. p-values < 0.05 were considered statistically significant.

Results

Microstructure of micronized cellular adipose matrix

After mouse, adipose tissue was morcellated (100–400 μm maximum dimension), suspended in PBS and centrifuged, tissues were separated into yellowish floating adipose tissue (floating fat) and whitish bottom sedimentation (MCAM) (Figure 1A, left). Scanning electron microscopy (SEM) confirmed a scarcity of adipocytes in MCAM, whereas adipocytes were abundant in floating fat (Figure 1A, right). The lobular structure of floating fat was maintained, with MCAM consisting primarily of connective tissue and collagen bundles.

Whole-mount imaging highlighted functional features of MCAM (Figure 1B). As noted by scanning electron microscopy, MCAM was lacking in mature adipocytes (i.e., the large, round WGA$^+$ (wheat germ agglutinin) green cells seen in floating fat). However, Hoechst$^+$ nucleated cells persisted in MCAM at rather high density. In addition, MCAM retained branches and segments of vessels and identifiable capillaries.

Cellular content of SVF isolated from mouse MCAM

Fluorescence-activated cell sorting analyses were performed to delineate cellular composition, once SVFs were individually isolated from floating fat and MCAM through collagenase digestion (Figure 2). SVFs of fat and MCAM were characterized through a combination of surface markers and classified into four subpopulations; hematopoietic cells (mainly white blood cells; CD45$^+$), vascular endothelial cells (CD45$^-$/CD31$^+$/CD34$^+$), ASCs (CD45$^-$/CD31$^-$/CD34$^+$), and other cells (CD45$^-$/CD31$^-$/CD34$^-$). The SVF of floating fat consisted largely of CD45$^-$ nonhematopoietic cells (~75%), with ASCs accounting for half of the nonhematopoietic fraction. The SVF of MCAM contained all four subpopulations (including ASCs) albeit in differing ratios. ASCs accounted for 13% of MCAM-SVF cells, with hematopoietic cells, vascular endothelial cells and other cells constituting 57.9, 0.7 and 28.3%, respectively. The original protocol was designed for optimal adipose digestion, which may explain the less efficient digestion of MCAM connective tissue and its different composition of cells (ASCs and vascular endothelial cells).

Multilineage differentiation capacity of ASCs isolated from human MCAM

MCAM and floating fat were also extracted from the human lipoaspirate. Cultured ASCs derived from human floating fat and MCAM were compared in terms of capacity for differentiating into three mesenchymal lineages: adipogenic, osteogenic and chondrogenic. After 3 weeks of induction, ASCs of both floating fat and MCAM displayed similar degrees of multilineage differentiation. No morphologic differences in Nile red, von Kossa or Alcian blue staining were detected (Figure 3A), nor did quantification of lipid content, calcium deposition and micromass diameter (reflecting adipogenesis, osteogenesis and chondrogenesis, respectively) differ significantly (Figure 3B). Thus, it was indicated that MCAM contained ASCs with similar differentiating capability to those obtained from regular adipose tissue.

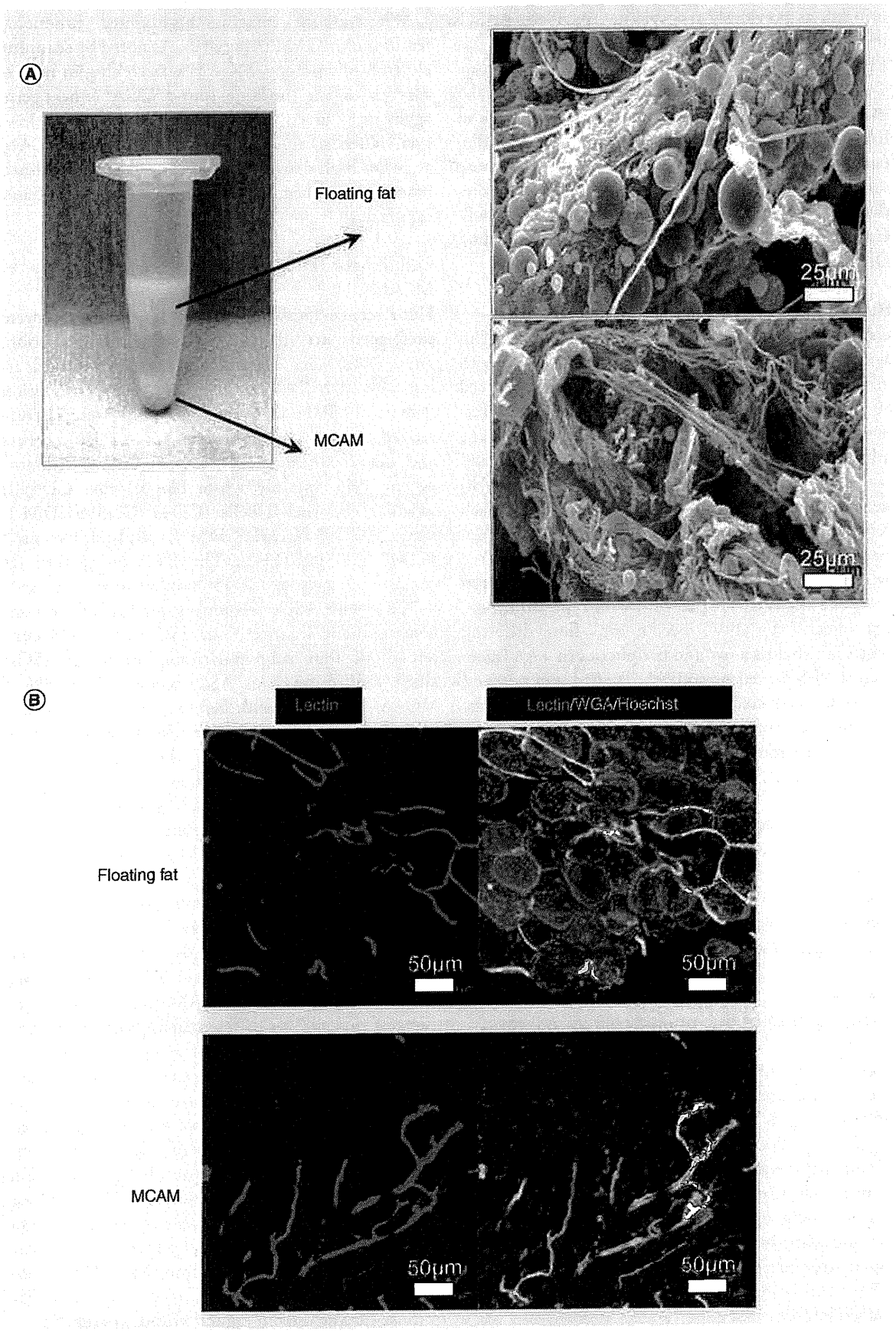
Ⓐ
Floating fat
MCAM
25μm
25μm
Ⓑ
Lectin
Lectin/WGA/Hoechst
Floating fat
MCAM
50μm
50μm
50μm
50μm

Figure 1. Microstructure of floating fat and micronized cellular adipose matrix (see facing page). (A) Once minced inguinal fat pad of mouse was centrifuged, micronized cellular adipose matrix (MCAM; whitish sediment) separated from floating fat. Scanning electron microscopy revealed highly fibrous nature of MCAM (vs floating fat), with few mature adipocytes. Bars = 25 μm. **(B)** Whole-mount staining of lectin (vascular endothelial cells: red), wheat germ agglutinin (cell membranes: green) and Hoechst (nuclei: blue); mature adipocytes scarce in MCAM, but microvascular structures in connective tissue remained intact. Bars = 50 μm.
MCAM: Micronized cellular adipose matrix; WGA: Wheat germ agglutinin.
For color images please see online at www.futuremedicine.com/doi/full/10.2217/RME.15.48

Therapeutic effects of mouse MCAM for diabetic ulcers

Subcutis of full-thickness dorsal skin ulcers inflicted in diabetic mice was injected at wound peripheries with MCAM prepared from wild-type mice, using pBS injections as control. Healing of diabetic ulcers was significantly more rapid with MCAM (vs pBS) injection, with 64% smaller wound size on day 4 ($p = 0.0082$) and 65% smaller size on day 7 ($p = 0.0043$; Figure 4). At the close of week 2, closure was essentially completed in MCAM-treated ulcers, whereas wound beds of pBS-treated ulcers remained hyperemic.

Discussion

For this investigation, our injectable MCAM by design was a formulation of bioactive ECM and functional ASCs, prepared by mechanical mincing and elimination of adipocytes from adipose tissue. Sharp-bladed instruments, such as scissors, easily micronized the connective tissue in fat without significantly altering its basic structure, and viability of cells was retained. Approximate specific gravities of human adipocyte and connective tissue obtained from human lipoaspirates were 0.85–0.87 and 1.1–1.2, respectively, underscoring that MCAM regularly sediments upon centrifugation of processed samples.

There is an abundance of evidence affirming the biologic utility of ECM, namely the capacity to regulate proliferation and differentiation of tissue-resident stem cells [14]. Acellular ECM products, whether dermal or fatty by nature, have proven therapeutic in clinical and experimental contexts [9–11,15–16], providing biocompatible substrates or scaffolding and trophic/growth factors needed to accommodate and recruit stem/progenitor cells. In addition to supplying ECM essentials, our MCAM injectable also incorporates an array of viable cells (ASCs, vascular endothelial cells and more) that engage in wound healing.

To date, such scaffolds are designed to mimic native environments, ensuring original cell functions are maintained for optimal cell expansion and tissue regeneration [17–19]. ASCs in MCAM occupy their original ECM niche, ready to assume original roles. As shown by whole-mount staining and flow cytometry, vessels and capillaries of MCAM, as well as ASCs and other stromal cells, retained their natural states and positions. Functional aspects of ASCs in MCAM were also well preserved, as partly indicated by differentiation assays.

ASCs are thought to be potent sources of trophic factors and to have multilineage differentiation capacity. Nonetheless, in transplantation of dissociated (suspended) ASCs, local retention was found to be poor (many disappearing in 1 week), thus nullifying therapeutic intent or resulting in unexpected stem cell behaviors [5,7,20]. As the size of injectable MCAM ranges 100–400 μm, the ECM of MCAM may also provide better mechanical support and anchorage for ASCs to avoid their rapid and seemingly detrimental migration.

Our *in vivo* results suggest that MCAM does impact the healing of diabetic ulcers by accelerating tissue repair. Although similar therapeutic effects have already been reported with use of isolated and cultured ASCs in diabetic or generic refractory ulcers [21–24], substantial procedural manipulations (i.e., enzymatic digestion and isolation or culture of cells) to possibly change biological properties of ASCs are not required for MCAM preparation, eliminating potential regulatory concerns. In skin wound healing models, significant differences are usually observed at a specific and limited time range [25,26], because the skin wound closes eventually in any model (thus no difference at later stages). Our objective was to design a safe and functional injectable, requiring little in the way of preparation. In this study, MCAM obtained from wild-type healthy mice was administered into diabetic mice and it is a limitation of this study that MCAM from diabetic mice was not evaluated. Although ASCs from diabetic patients may not have the same function as those from healthy subjects, ASCs are known to be relatively immunoprivileged and may work as a temporary drug to release trophic factors and help wound healing by allogeneic use.

Fat grafting is claimed to have comparable clinical effects, promoting wound healing of refractory ulcers, such as those seen postirradiation [27–29], and providing a remedy for stem-cell depleted conditions such as chronic ischemia [30,31], systemic sclerosis [32] and scar contracture [33–35]. Improvement of such problematic conditions suggests that the clinical benefits may be partly attributable to functional ASCs. However, if volumetric restoration is not desired, as in transplantations for tissue revitalization/fertilization, the volume occupied by adipocytes within the graft would signifi-

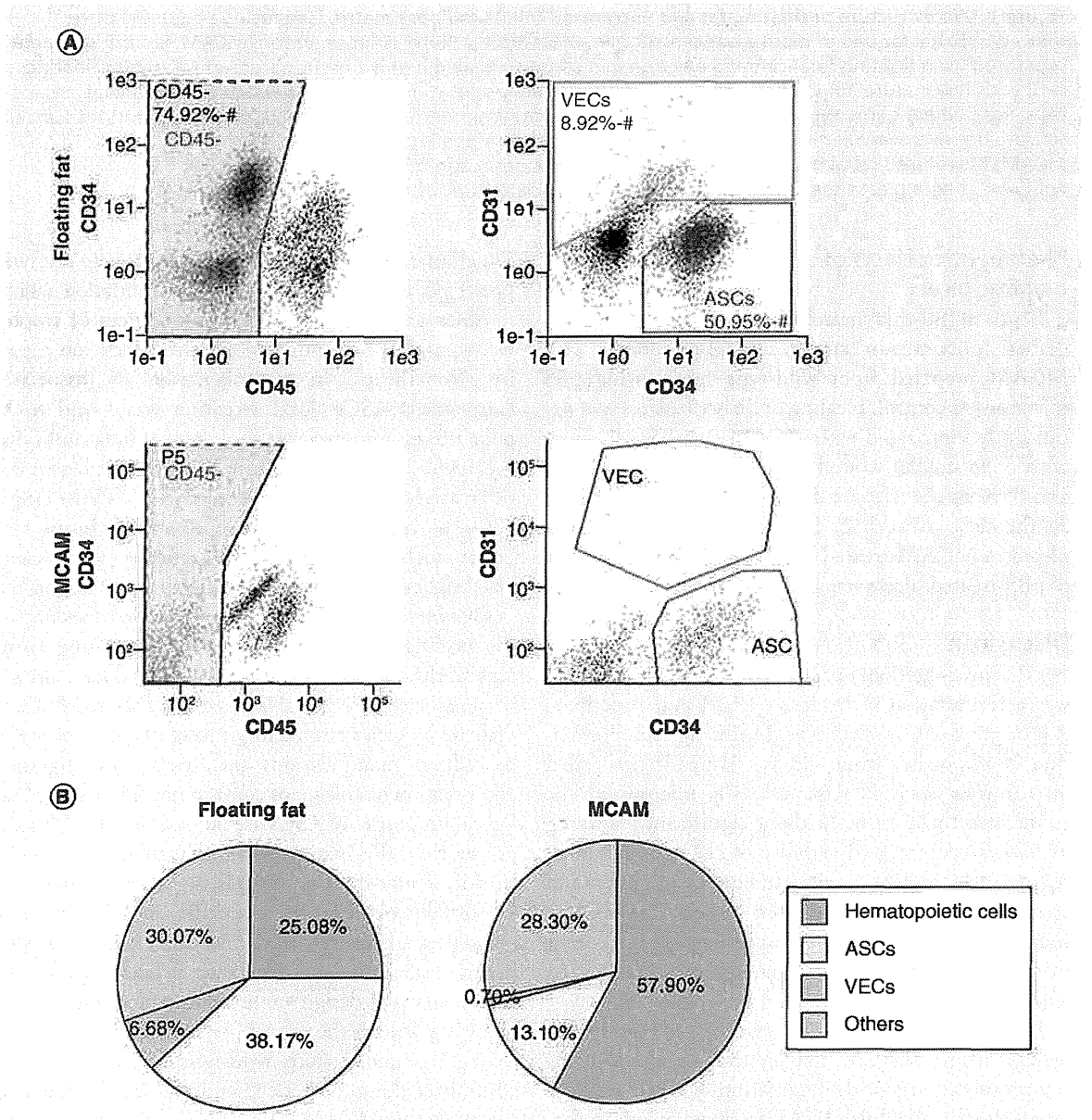

Figure 2. Cellular content of stromal vascular fraction isolated from mouse floating fat and micronized cellular adipose matrix. (A) SVFs from floating fat and that from MCAM were isolated through digestion by collagenase, identifying content as follows: hematopoietic cells (primarily WBCs; $CD45^+$), VECs ($CD45^-/CD31^+/CD34^+$), ASCs ($CD45^-/CD31^-/CD34^+$) and other cells ($CD45^-/CD31^-/CD34^-$). **(B)** ASCs in MCAM account for 13.1% of SVF cells. Hematopoietic cells, VECs and other cells comprise 57.9, 0.7 and 28.3%, respectively. More ASCs (38.2%) and VECs (6.7%) are evident in SVF of floating fat by comparison.
ASC: Adipose-derived stem/stromal cell; MCAM: Micronized cellular adipose matrix; SVF: Stromal vascular fraction; VEC: Vascular endothelial cell.

cantly decrease the density of ASCs and ECM. In these cases, ASCs alone or in conjunction with ECM (as in MCAM) may provide sufficient therapeutic effect, as we have shown.

Conclusion

MCAM is an autologous/allogeneic injectable of bioactive ECM and functional cellular components generated through minimal manipulation of adipose tissue. Smaller-sized and more homogeneous (50–100 μm) particles may be preferable as injectables, but as we already learned, such preparations may jeopardize the viability of cells. Further studies are needed to verify the hypothesized mechanism underlying the efficacy of MCAM and further optimization of preparation methods. Therapeutic effect of MCAM in other stem

cell-depleted states, including irradiation damage and fibrous diseases will also need to be tested. Besides, we still need to elucidate the specific functions of adipocytes in clinical fat grafting and to see what benefits of fat grafting will be lost when we use the product like MCAM, where mature adipocytes are virtually absent. Our efforts here attest to the therapeutic potential of MCAM in ischemic diabetic ulcers, offering a novel mode of tissue repair and revitalization with a minimally invasive approach.

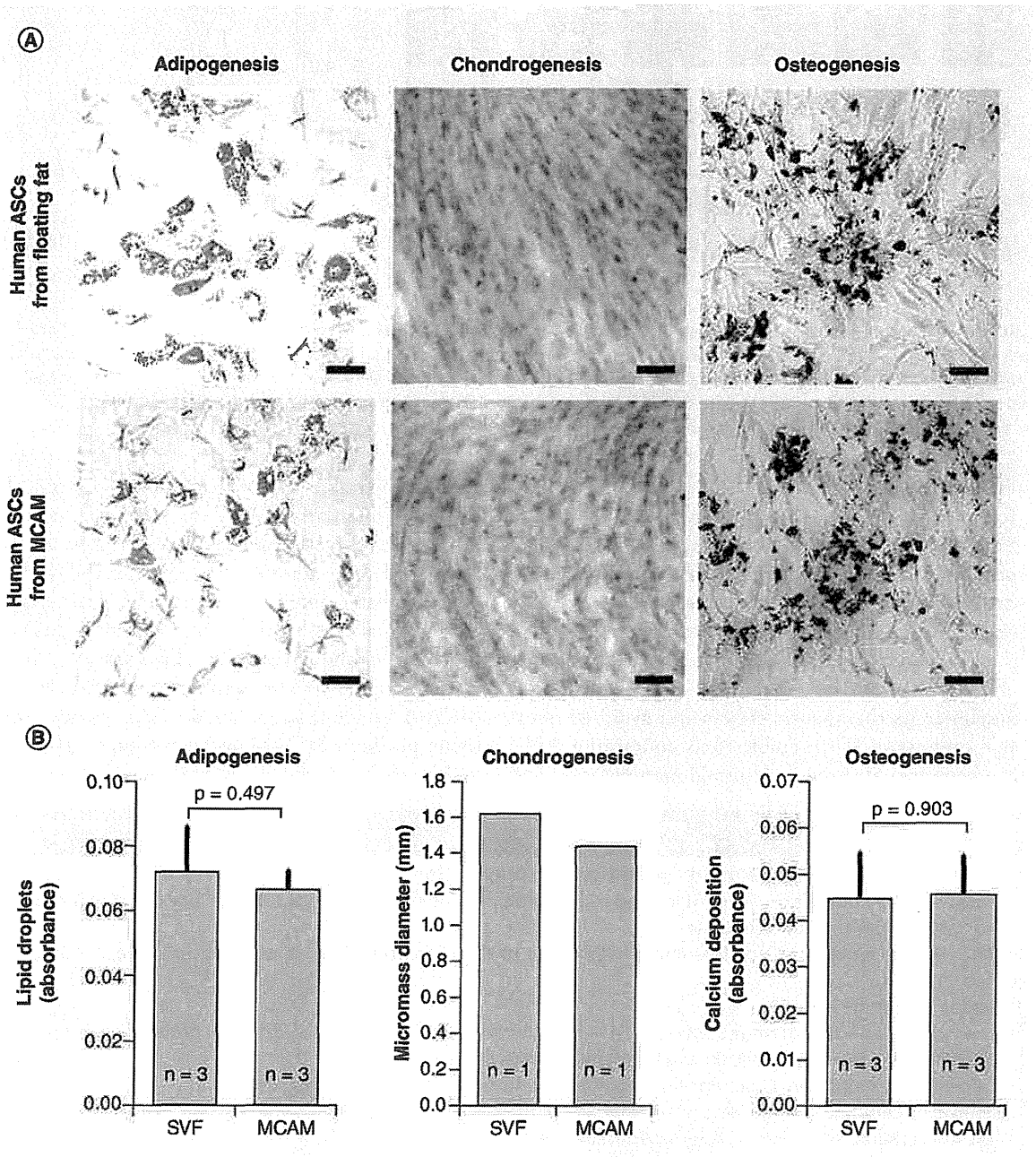

Figure 3. Multilineage differentiation capacity of cultured adipose-derived stem/stromal cells isolated from human floating fat and micronized cellular adipose matrix. (A) Microscopic images of differential induction: cultured human ASCs of floating fat and MCAM yielded similar adipogenic, chondrogenic and osteogenic differentiation; lineage-specific differentiation delineated by Nile red, Alcian blue and von Kossa stains, respectively. Scale bar = 100 μm. **(B)** Quantitative analysis of cellular differentiation: capacity for multilineage differentiation, as indicated by accumulated lipid (adipogenesis), micromass diameter (chondrogenesis) and calcium deposition (osteogenesis), showing no significant differences between fractions. ASC: Adipose-derived stem/stromal cell; MCAM: Micronized cellular adipose matrix; SVF: Stromal vascular fraction.

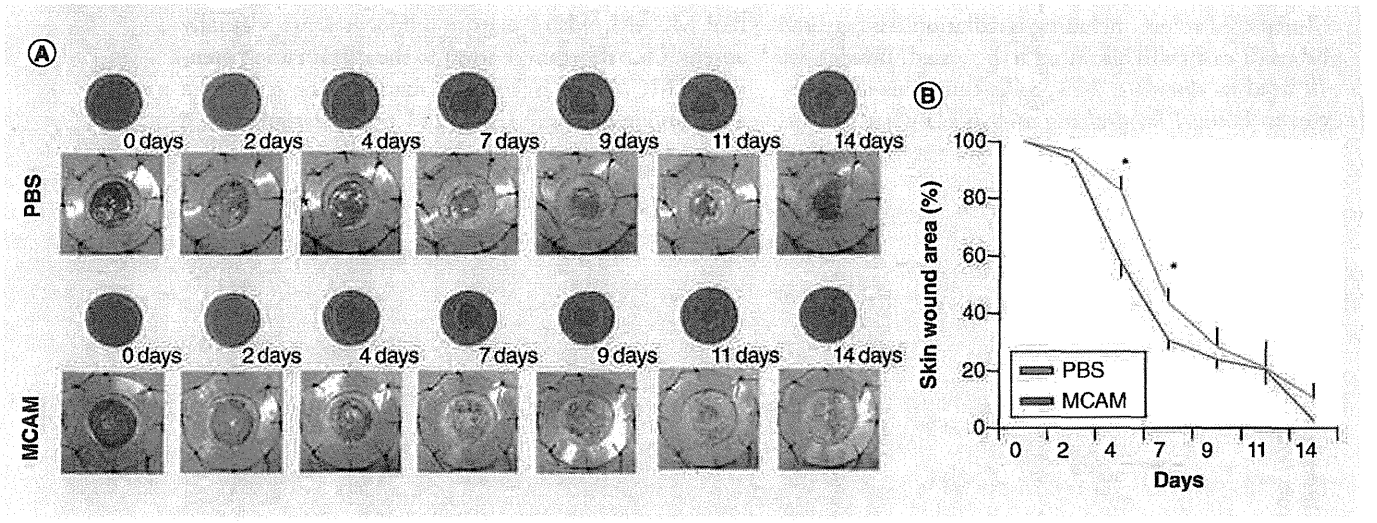

Figure 4. Therapeutic mouse micronized cellular adipose matrix injection of diabetic ulcers. (A) Representative photos of cutaneous wounds (6 mm) created on dorsal areas of diabetic (db/db) mice (n = 4) and treated by local injection of PBS or MCAM on day 0, with 2-week follow-up; ulcerated surface areas determined via software. **(B)** Comparison of wound surface areas (determined digitally): significantly reduced ulcer size in MCAM-injected mice (vs PBS-injected controls), day 4 ($p = 0.0082$) and day 7 ($p = 0.0432$).
MCAM: Micronized cellular adipose matrix; PBS: Phosphate-buffered saline.

Future perspective

Regulatory organizations in many countries regard SVF isolated from adipose tissue as a 'more than minimal manipulated' biological drug, of which uses are strictly regulated due to its associated safety issues. Although therapeutic potential of ASCs in the SVF was extensively studied, cell suspension of ASCs may not be the optimal means in order to maximize its therapeutic effects and avoid unfavorable migration. If injectable tools containing ASCs can be prepared through minimal manipulation and show comparable therapeutic effects, it would be a potential alternative. Also, as ASCs are relatively immunoprivileged, allogeneic ASCs may be clinically used, for example, as a temporarily-working drug to release cytokines. It may be a good news for diseased patients whose ASCs cannot function as those of healthy patients. In this study, we focused on the characterization and therapeutic effects of MCAM as the first step to develop a new cellular/tissue product. MCAM accommodates viable ASCs within their natural niche and may be valuable in

Executive summary

Micronized cellular adipose matrix definition and preparation

- MCAM is the abbreviation for micronized cellular adipose matrix. It is an injectable cellular matrice product extracted from the adipose tissue.
- MCAM is obtained as the pelleted material from centrifugation after finely mincing and fragmentation of fat tissue.

Microstructure of MCAM

- Comparing with the intact fat tissue, MCAM includes few adipocytes but a substantial number of adipose derived stem cells (ASCs) within its abundant connective tissue.
- Microvascular structures in extracellular connective tissue of MCAM remained intact.

Analysis of cellular composition

- MCAM retained ASCs and vascular endothelial cells.
- ASCs within MCAM were viable and maintained similar mesenchymal differentiation capacity compared to those ASCs obtained through the standard collagenase digestion method.

Regenerative potential

- In diabetic mice model, excisional skin wounds treated with MCAM showed accelerated healing compared to phosphate-buffered saline-treated wounds.

Conclusion

- MCAM is an injectable tissue product contains both functional stem cells and extracellular matrix. MCAM is prepared through minimal manipulation and thus can be readily used without regulatory issues. MCAM may offer a safe and effective option in chronic wound repair and tissue revitalization.

treating stem cell-depleted conditions such as chronically inflammated tissues/ulcers and radiated tissue damage. Another future study is needed to explore the effectiveness of MCAM compared with other cellular formulations such as freshly isolated SVF and cultured ASCs.

Financial & competing interests disclosure

This study was supported by the Japanese Ministry of Education, Culture, Sports, Science and Technology (MEXT); contract grant number: Grant-in-Aid for Scientific Research B3-24390398. The authors have no other relevant affiliations or financial involvement with any organization or entity with a financial interest in or financial conflict with the subject matter or materials discussed in the manuscript apart from those disclosed.

No writing assistance was utilized in the production of this manuscript.

Ethical conduct of research

The authors state that they have obtained appropriate institutional review board approval or have followed the principles outlined in the Declaration of Helsinki for all human or animal experimental investigations. In addition, for investigations involving human subjects, informed consent has been obtained from the participants involved.

References

Papers of special note have been highlighted as:
• of interest

1 Yoshimura K, Suga H, Eto H. Adipose-derived stem/progenitor cells: roles in adipose tissue remodeling and potential use for soft tissue augmentation. *Regen. Med.* 4(2), 265–273 (2009).

2 Yoshimura K, Eto H, Kato H *et al. In vivo* manipulation of stem cells for adipose tissue repair/reconstruction. *Regen. Med.* 6(6 Suppl.), 33–41 (2011).

3 Gentile P, Orlandi A, Scioli MG *et al.* A comparative translational study: the combined use of enhanced stromal vascular fraction and platelet-rich plasma improves fat grafting maintenance in breast reconstruction. *Stem Cells Transl. Med.* 1(4), 341–351 (2012).

4 Kølle SF, Fischer-Nielsen A, Mathiasen AB *et al.* Enrichment of autologous fat grafts with *ex-vivo* expanded adipose tissue-derived stem cells for graftsurvival: a randomised placebo-controlled trial. *Lancet* 382(9898), 1113–1120 (2013).

5 Yoshimura K, Aoi N, Suga H *et al.* Ectopic fibrogenesis induced by transplantation of adipose-derived progenitor cell suspension immediately after lipoinjection. *Transplantation* 85(12), 1868–1869 (2008).

• **A clinical report of unfavorable stem cell migration and differentiation called for attention to the possible risk of local injection of stromal vascular fraction cell suspension.**

6 Yamada Y, Nakamura S, Ito K *et al.* Injectable tissue-engineered bone using autogenous bone marrow-derived stromal cells for maxillary sinus augmentation: clinical application report from a 2–6-year follow-up. *Tissue Eng. Part A* 14(10), 1699–1707 (2008).

7 Cheng NC, Wang S, Young TH. The influence of spheroid formation of human adipose-derived stem cells on chitosan films on stemness and differentiation capabilities. *Biomaterials* 33(6), 1748–1758 (2012).

8 Matsuura K, Utoh R, Nagase K *et al.* Cell sheet approach for tissue engineering and regenerative medicine. *J. Control. Release* 190, 228–239 (2014).

9 Vorotnikova E, McIntosh D, Dewilde A *et al.* Extracellular matrix-derived products modulate endothelial and progenitor cell migration and proliferation *in vitro* and stimulate regenerative healing *in vivo*. *Matrix Biol.* 29(8), 690–700 (2010).

10 Novitsky YW, Rosen MJ. The biology of biologics: basic science and clinical concepts. *Plast. Reconstr. Surg.* 130(5 Suppl. 2), S9–S17 (2012).

11 Iorio ML, Shuck J, Attinger CE. Wound healing in the upper and lower extremities: a systematic review on the use of acellular dermal matrices. *Plast. Reconstr. Surg.* 130(5 Suppl. 2), S232–S241 (2012).

12 Halme DG, Kessler DA. FDA regulation of stem-cell-based therapies. *N. Engl. J. Med.* 355(16), 1730–1735 (2006).

13 Umeda K, Zhao J, Simmons P *et al.* Human chondrogenic paraxial mesoderm, directed specification and prospective isolation from pluripotent stemcells. *Sci. Rep.* 2, 455 (2012).

14 Discher DE, Mooney DJ, Zandstra PW. Growth factors, matrices, and forces combine and control stem cells. *Science* 324(5935), 1673–1677 (2009).

15 Choi JS, Yang HJ, Kim BS *et al.* Fabrication of porous extracellular matrix scaffolds from human adipose tissue. *Tissue Eng. Part C Methods* 16(3), 387–396 (2010).

• **The study first showed the function and potential use of decellularized extracellular matrix from adipose tissue for regenerative medicine.**

16 Sano H, Orbay H, Terashi H *et al.* Acellular adipose matrix as a natural scaffold for tissue engineering. *J. Plast. Reconstr. Aesthet. Surg.* 67(1), 99–106 (2014).

17 Li Y, Liu W, Liu F *et al.* Primed 3D injectable microniches enabling low-dosage cell therapy for critical limb ischemia. *Proc. Natl Acad. Sci. USA* 111(37), 13511–13516 (2014).

18 Lin CS, Xin ZC, Deng CH *et al.* Defining adipose tissue-derived stem cells in tissue and in culture. *Histol. Histopathol.* 25(6), 807–815 (2010).

19 Yang G, Rothrauff BB, Lin H *et al.* Enhancement of tenogenic differentiation of human adipose stem cells by tendon-derived extracellular matrix. *Biomaterials* 34(37), 9295–9306 (2013).

20 Park IS, Chung PS, Ahn JC. Enhanced angiogenic effect of adipose-derived stromal cell spheroid with low-level light therapy in hind limb ischemia mice. *Biomaterials* 35(34), 9280–9289 (2014).

21 Amos PJ, Kapur SK, Stapor PC *et al.* Human adipose-derived stromal cells accelerate diabetic wound healing: impact of cell formulation and delivery. *Tissue Eng. Part A* 16(5), 1595–1606 (2010).

22 Tanaka R, Vaynrub M, Masuda H *et al.* Quality-control culture system restores diabetic endothelial progenitor cell vasculogenesis and accelerates wound closure. *Diabetes* 62(9), 3207–3217 (2013).

23 Ebrahimian TG, Pouzoulet F, Squiban C *et al.* Cell therapy based on adipose tissue-derived stromal cells promotes physiological and pathological wound healing. *Arterioscler. Thromb. Vasc. Biol.* 29(4), 503–510 (2009).

24 Han SK, Kim HR, Kim WK. The treatment of diabetic foot ulcers with uncultured, processed lipoaspirate cells: a pilot study. *Wound Repair Regen.* 18(4), 342–348 (2014).

25 Kim EK, Li G, Lee TJ *et al.* The effect of human adipose-derived stem cells on healing of ischemic wounds in a diabetic nude mouse model. *Plast. Reconstr. Surg.* 128(2), 387–394 (2011).

26 Zografou A, Papadopoulos O, Tsigris C *et al.* Autologous transplantation of adipose-derived stem cells enhances skin graft survival and wound healing in diabetic rats. *Ann. Plast. Surg.* 71(2), 225–232 (2013).

27 Rigotti G, Marchi A, Galiè M *et al.* Clinical treatment of radiotherapy tissue damage by lipoaspirate transplant: a healing process mediated by adipose-derived adult stem cells. *Plast. Reconstr. Surg.* 119(5), 1409–1422 (2007).

28 Phulpin B, Gangloff P, Tran N *et al.* Rehabilitation of irradiated head and neck tissues by autologous fat transplantation. *Plast. Reconstr. Surg.* 123(4), 1187–1197 (2009).

29 Salgarello M, Visconti G, Barone-Adesi L. Fat grafting and breast reconstruction with implant: another option for irradiated breast cancer patients. *Plast. Reconstr. Surg.* 129(2), 317–329 (2012).

30 Klinger M, Caviggioli F, Vinci V *et al.* Treatment of chronic posttraumatic ulcers using autologous fat graft. *Plast. Reconstr. Surg.* 126(3), e154–e155 (2010).

31 Marangi GF, Pallara T, Cagli B *et al.* Treatment of early-stage pressure ulcers by using autologous adipose tissue grafts. *Plast. Surg. Int.* 2014, 817283 (2014).

32 Del Papa N, Caviggioli F, Sambataro D *et al.* Autologous fat grafting in the treatment of fibrotic perioral changes in patients with systemic sclerosis. *Cell Transplant.* 24(1), 63–72 (2015).

33 Caviggioli F, Maione L, Forcellini D *et al.* Autologous fat graft in postmastectomy pain syndrome. *Plast. Reconstr. Surg.* 128(3), 349–352 (2011).

34 Mazzola IC, Cantarella G, Mazzola RF. Management of tracheostomy scar by autologous fat transplantation: a minimally invasive new approach. *J. Craniofac. Surg.* 24(4), 1361–1364 (2013).

35 Pallua N, Baroncini A, Alharbi Z *et al.* Improvement of facial scar appearance and microcirculation by autologous lipofilling. *J. Plast. Reconstr. Aesthet. Surg.* 67(8), 1033–1037 (2014).